Catalysis Today 166 (2011) 84–90

Contents lists available at ScienceDirect

Catalysis Today

journal homepage: www.elsevier.com/locate/cattod

RE_2O_3-promoted Pt–SO_4^{2-}/ZrO_2–Al_2O_3 catalyst in *n*-hexane hydroisomerization

G.X. Yu[a,b], D.L. Lin[b], Y. Hu[b], X.L. Zhou[b,*], C.L. Li[b], L.F. Chen[c], J.A. Wang[c]

[a] School of Chemistry and Environmental Engineering, Jianghan University, Wuhan 430056, China
[b] School of Chemical Engineering, East China University of Science & Technology, Shanghai 200237, China
[c] ESIQIE, Instituto Politécnico Nacional, Av. Politécnico S/N, Col. Zacatenco, 07738 México, D.F., Mexico

ARTICLE INFO

Article history:
Available online 11 July 2010

Keywords:
Rare earth oxide promotion
Hydroisomerization
n-Hexane
Sulfated zirconia
Alumina
Sulfate loss
Catalytic stability

ABSTRACT

Lanthanum, cerium and ytterbium nitrates used as RE oxide precursors, RE_2O_3-promoted PSZA catalysts for *n*-hexane hyroisomerization were prepared and RE_2O_3 promotion effects on catalytic activity and catalytic stability were investigated by N_2-adsorption, XRD, TG, FTIR, XPS and H_2-TPR. It was elucidated that the introduction of RE_2O_3 into Pt–SO_4^{2-}/ZrO_2–Al_2O_3 (PSZA) increased both the surface area and the number of active sites, resulting in a higher *n*-hexane isomerization activity. At the same time the catalyst stability has also been markedly increased by alleviating the sulfur loss and by stabilizing ZrO_2 tetragonal crystalline structure. In addition, XPS for the spent catalysts showed during *n*-hexane hydroisomerization reaction a relative small amount of S^{6+} species was reduced to S^{4+}, and the amount of the most active sulfate entities decided the overall amount of *n*-hexane transformed, their reduction being, perhaps, retarded by the RE_2O_3 addition to PSZA. The promotion effects of RE oxides addition decreased in the order: $La_2O_3 > Yb_2O_3 > Ce_2O_3$.

1. Introduction

Crude oil contains about 10% light naphtha that is mainly composed of normal pentane (n-C_5) and normal hexane (n-C_6). Isomerization of n-C_5 and n-C_6 has been recognized to be one of the most economical units to boost up octane level especially for the lower boiling end of gasoline. Owing to the environmental limitations on olefins and aromatics, light isoalkanes are considered to be very "clean" gasoline compositions. Hexane in reforming feedstock mainly converts to benzene by dehydrocyclization. Benzene is both toxic and carcinogenic and therefore is limited to no more than 1% in gasoline with the total aromatics capped at approximately 25% from this decade. Therefore *n*-hexane is nowadays preferably used as isomerization feedstock to produce gasoline [1,2].

In the early years, liquid superacids such as SbF_5/HF or SbF_5/HSO_3F were used as isomerization catalysts that operated at low temperatures up to 0 °C [3]. However, these liquid superacids were later abandoned, because they were corrosive and difficult to be recovered and treated. Two types of solid catalysts were then be commercially used for naphtha isomerization. The first was platinum on chlorided alumina catalyst used in the Penex process that provided isomers with about 83 RON at lower temperature around 140 °C for C_5 feed. However it required the continuous addition of chloride to maintain the acidity necessary for a high catalytic activity. This acid environment requires careful drying of feedstock and causes corrosion as well as pollution problems in the event of operational upset. Moreover, this kind of catalyst was very sensitive to sulfur in the feedstock. The other was Pt/zeolite catalysts used in the so-called Hysomer process that would not suffer from above disadvantages, whilst requires operating temperatures higher than 250 °C and thus produces gasoline with RON of only 78 as a consequence of the thermodynamic limitations [4]. In the last two decades, anion modified metal oxides, like sulfated zirconia (SZ), have attracted significant attention due to their high activities, their less sensitivity to the impurities and no corrosion or pollution problems [5]. Nevertheless, it was usually observed that SZ showed rapid deactivation [1,6,7]. Such deactivation occurs as a consequence of: (1) coke deposition or formation of unsaturated surface deposits [8] and (2) sulfur surface complex oxidation states' reduction [9,10]. A number of transition metals promoters (e.g. Fe, Mn, and Ni) have been added to SZ, resulting in catalysts with higher activity than unmodified SZ [11]. However, rapid deactivation was still observed [12–14] and the marked promoting effect disappeared if the reaction was performed at temperatures higher than 250 °C [15,16].

Incorporation of alumina and platinum to SZ to prepare Pt–Al-promoted SZ (PtSZA) catalysts is a key achievement for it to be industrially applied in hexane hydroisomerization. Initially it was concluded that loading of platinum on sulfated zirconia (SZ) to form a PtSZ catalyst would only significantly inhibit the forma-

* Corresponding author at: School of Chemical Engineering, East China University of Science & Technology, 130, Meilong Road, Shanghai 200237, China.
Tel.: +86 21 64252041; fax: +86 21 64253049.
E-mail addresses: xiaolong@ecust.edu.cn, pprc_zy@ecust.edu.cn (X.L. Zhou).

0920-5861/$ – see front matter © 2010 Elsevier B.V. All rights reserved.
doi:10.1016/j.cattod.2010.06.005

tion of coke and thus improve the stability [17]. Meanwhile, SZ catalysts were in powdered form and the mechanical properties of pure extrudates were very poor, therefore mixing with an alumina binder was necessary to prepare an industrial hydroisomerization catalyst like Pt/ZSA. It has been confirmed that the introduction of a small amount of alumina could improve SZA catalyst activity and stability for alkane hydroisomerization [15,18–22]. Platinum was also reported to be a good promoter to increase acidity as well as dehydrogenation–hydrogenlation ability and therefore Pt may improve the activity for alkane isomerization [23]. In the present work lanthanum, cerium and ytterbium nitrates were used as RE oxide precursors with the purpose of enhancing the catalysts stability. RE_2O_3-promoted PSZA catalysts were prepared and the promotion effects on the activity and selectivity are reported using *n*-hexane hydroisomerization as a test reaction.

2. Experimental

2.1. Catalyst preparation

A solution with zirconium content of 0.4 mol/L was prepared by dissolving $ZrOCl_2{\cdot}8H_2O$ in deionized water. A 26 wt.% ammonia solution was dropwise added into that solution at a rate of 0.5 mL/min up to pH of 10. The precipitate was filtered after being aged for 24 h at 60 °C. The precipitate was washed with distilled water until the disappearance of chloride ions ($AgNO_3$ test), dried at 110 °C for 12 h. The obtained $Zr(OH)_4$ sample was shaped with boehmite (76.2 wt.% alumina; pore volume, 0.342 mL/g; surface area, 273 m^2/g), and alumina content in the mixture is 5 wt.%. The latter was dried at 110 °C and then pulverized to particles smaller than 290 μm, and then the dry solid was separated into two portions.

One portion was sulfated by impregnation method with 0.5 mol/L of H_2SO_4 solution (15 mL/g) under continuous stirring at room temperature for 12 h. The sulfated boehmite-$Zr(OH)_4$ was filtered without washing then dried overnight at 110 °C, and then the dry sulfated solid was calcined at 625 °C for 3 h. Subsequently, the above products were impregnated with H_2PtCl_6 solution for 24 h at ambient temperature using the incipient wetness technique. It was then dried overnight at 110 °C before the final calcination at a fixed temperature of 525 °C for 2 h. The platinum content was 0.5 wt.%. The obtained Pt–SO_4^{2-}/ZrO_2–Al_2O_3 catalysts were designated as PSZA.

The other portion was impregnated with 1.5 mol/L of rare earth nitrate solutions using the incipient wetness technique at ambient temperature for 24 h. Zr/RE (molar ratio) is 100. Rare earth nitrates are lanthanum, cerium and ytterbium nitrates. The solids were dried, and then sulfur was loaded by mixing with 0.5 mol/L H_2SO_4 and 15 mL/g solid. For our catalyst preparation, the sulfating process is the same for all catalysts. Finally they were dried and calcined at 625 °C for 3 h. Subsequently, the SO_4^{2-}/ZrO_2–Al_2O_3–RE_2O_3 catalysts were impregnated with H_2PtCl_6 solution using the incipient wetness method as described above. They were then dried overnight at 110 °C before the final calcination at a fixed temperature of 525 °C for 2 h. The platinum content was 0.5 wt.%. The obtained catalysts were respectively designated as PSZAC, PSZAL and PSZAY.

2.2. Catalyst characterization

The surface areas and pore diameters of the catalysts were measured by N_2 adsorption–desorption isotherms at −196 °C with a Mircomeritics ASAP 2010 instrument. Prior to analysis, each sample was degassed at 200 °C for 6 h under 10^{-3} Torr. Specific surface areas were calculated by BET method and the pore size distribution patterns were obtained from the analysis of the desorption portion of the isotherms using the BJH method.

Table 1
Textural structure of catalysts.

Catalyst	BET surface area (m^2/g)	Pore volume (mL/g)	Average pore diameter (nm)
PSZA	117.5	0.1764	6.24
PSZAC	129.1	0.1558	4.99
PSZAL	135.2	0.1646	5.04
PSZAY	124.5	0.1568	5.22

The powder X-ray diffraction (XRD) patterns were recorded on a Rigaku D/Max 2550 X using Cu Kα (l = 0.154 nm) radiation in an operating mode of 40 kV and 30 mA. Data were collected in a 2θ range between 20° and 70° in steps of 0.02°/s.

Thermogravimetric analyses (TG) were performed on a SDT-Q600 instrument (TA, USA) in flowing air with temperature ramp set at 5 °C/min in the 25–1000 °C temperature range.

Fourier-transform infrared (FTIR) spectra of adsorbed pyridine were recorded on a Bruker IES-88 spectrometer. The sample was pressed to a 15 mm plate and put in a wafer. It was degassed in vacuum of 10^{-4} Torr at 450 °C for 2 h and lowered the temperature to 200 °C. Pyridine was adsorbed for 10 min and took 30 min for equilibrium. The adsorption system was vacuumed for 40 min. Then the temperature was raised to 300 °C. Same procedures were performed for 400 °C and 450 °C. The IR spectra were recorded after 10 min for equilibrium at desired temperature. The number of Brønsted and Lewis acid sites was calculated according to the integral area of the bands at 1540 cm^{-1} and 1450 cm^{-1}, respectively.

H_2-temperature programmed reduction (TPR) experiments were performed in Auto Chem II (Micromeritics, USA). The heating rate was 10 °C/min from 50 °C to 900 °C using argon stream containing 7 vol.% hydrogen. The hydrogen consumption was measured by a Shimadzu GC-8A gas chromatograph, equipped with a thermal conductivity detector (TCD).

X-ray photoelectron spectroscopy (XPS) spectra were recorded on a Kratos Axis Ultra DLD spectrometer equipped with AlKα X-ray source (1486.6 eV).

2.3. Catalytic activity measurements

The *n*-hexane hydroisomerization reaction was carried out in a flow-type fixed-bed reactor loaded with 1.0 g of catalyst. Prior to the reaction, the catalyst sample was pre-treated with flowing dry air (40 mL/min) at 450 °C for 3 h to remove water adsorbed on the surface. The system was cooled to 250 °C and the catalyst was reduced in flowing hydrogen for 3 h at 250 °C. Hydrogen and *n*-hexane mixture was then introduced into the reactor and hydroisomerization evaluations were performed under a total pressure of 2.0 MPa at desired temperature with *n*-hexane weight hourly space velocity (WHSV) of 1.0 h^{-1} and a hydrogen/*n*-hexane molar ratio of 5. Product compositions were monitored and analyzed using an on-line GC-920 temperature-programmed gas chromatograph with FID detector and 50-m OV-101 capillary column.

3. Results and discussion

3.1. Textural structures

Textural data of these four catalysts were listed in Table 1. The RE_2O_3-promoted catalysts developed a bigger surface area relative to PSZA, and BET surface area decreased in the order as: PSZAL > PSZAY > PSZAC > PSZA. Changes in the surface area of these catalysts are mainly observed at the calcination step for loading sul-

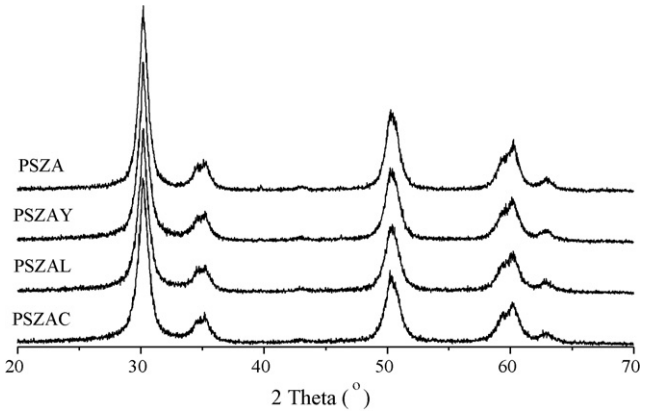

Fig. 1. XRD patterns of the catalysts.

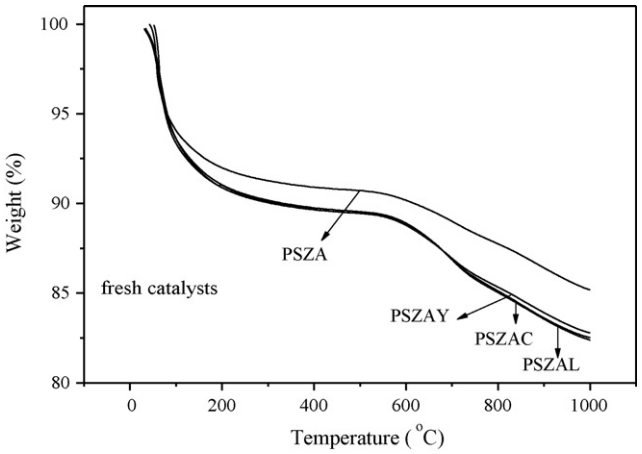

Fig. 2. TG curves of the catalysts.

fur species in catalyst preparation, which is necessary to produce superacid structures; meanwhile it would lead to drastic surface area decrease [6,7]. These results from Table 1 demonstrated that RE_2O_3 addition probably alleviated the catalyst sintering to retain higher surface area. In addition, decrease both in pore volume and average pore diameter after RE_2O_3 introduction was also observed, probably resulting from the coverage of RE_2O_3 on the inner surface of the catalyst. The doping of RE_2O_3 preventing the sintering of PSZA can only remain the surface area maximum as the same as the undoped sample, but cannot increase the surface area. Therefore, highly dispersed REO_3 on the surface of the sample might be responsible for the increment of the surface area. Of course, the enhancement of catalyst surface area would give favorable effect on catalytic activity.

3.2. XRD analysis

It has been generally realized that the crystalline phase of the SZ catalysts plays a very important role in catalytic activity and zirconia with tetragonal structure showing a higher catalytic activity than that of monoclinic ZrO_2 in alkane isomerization [24,25]. XRD patterns for crystalline structure characterization of PSZA and RE_2O_3-promoted PSZA catalysts were shown in Fig. 1. It was seen that these four catalysts had the peaks at 2θ of 30°, 35°, 50°, 60° and 63° respectively, and the peaks were assigned to tetragonal phases of zirconia which are active crystalline phases, whilst no any peaks corresponding to RE_2O_3 appeared. In other words, on the catalyst surfaces, RE_2O_3 species have been well dispersed and the crystalline phase structures of PSZA were kept unchanged after modification by rare earth RE_2O_3.

3.3. TG analysis

Thermal analysis results for PSZA and RE_2O_3-promoted PSZA catalysts after calcination were presented in Fig. 2. The TG curves of the four catalysts exhibited several weight loss stages. The first weight loss stage between 100 °C and 200 °C, was resulted from the removal of physically adsorbed water; the second weight loss stage, ranging from 200 °C to 550 °C, was related to dehydroxylation step. In the third stage, the weight loss between 550 °C and 620 °C corresponded to zirconia crystallization procedure. In the last stage in a temperature range between 620 °C and 1000 °C, the weight loss was due to decomposition of sulfates [26,27]. The corresponding weight losses in the last stage were around 4.79 wt.% for PSZA, around 6.19 wt.% for PSZAC, around 6.08 wt.% for PSZAL and around 5.70 wt.% for PSZAY. These data showed that RE_2O_3 addition increased sulfates content of PSZA. From the above results and BET data in Table 1, RE_2O_3 addition enhanced BET surface area of PSZA; it was concluded that introduction of RE_2O_3 into the catalyst resulted in a higher sulfates content that would alleviate the catalyst sintering and higher catalyst surface area.

3.4. Surface acidity

FTIR characterization of pyridine adsorption was applied to determine the numbers of Lewis and Brønsted acid sites between 200 °C and 400 °C on the PSZA and RE_2O_3-promoted PSZA catalysts. Results were presented in Table 2, where three kinds of acid sites with varying strengths were separated. The acid sites measured at 200 °C were assigned to weak acid sites, those at 300 °C were moderately strong acid sites, whereas that at 400 °C were assigned to superacid sites.

RE_2O_3 addition resulted in the increase of total acid sites. For weak acid sites, the introduction of La_2O_3 and Ce_2O_3 into PSZA only resulted in the increase of Brønsted acid sites, especially La_2O_3; however, Yb_2O_3 addition increased both Brønsted and Lewis acid sites. For moderately strong acid sites, the three RE_2O_3 addition led to the increase of both Brønsted and Lewis acid sites,

Table 2
Acidity data of the catalysts from FTIR spectra of adsorbed pyridine.

Desorb. temperature (°C)	Acid amount (μmol/g)	PSZA	PSZAC	PSZAL	PSZAY
200	B-Acid	28.3	33.4	46.1	56.8
	L-acid	65	60	62.3	96.6
	Tot-acid	93.3	93.4	108.4	153.4
300	B-Acid	15.4	24.5	42.3	35.1
	L-acid	31	34.8	51.1	38.7
	Tot-acid	46.4	59.3	93.4	73.8
400	B-Acid	4.2	8.6	17.7	17.7
	L-acid	14.4	14.1	28.6	18.9
	Tot-acid	18.6	22.7	46.3	36.6

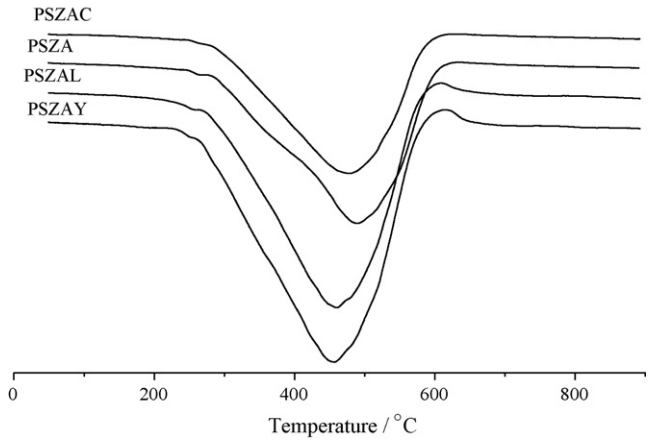

Fig. 3. H_2-TPR profiles of the catalysts.

and the increase deceased in the order: $La_2O_3 > Yb_2O_3 > Ce_2O_3$, and the increase of Brønsted acid sites was more obvious. For superacid sites, RE_2O_3 addition obviously increased Brønsted acid sites, Yb_2O_3 and La_2O_3 promotion was more obvious; Yb_2O_3 and La_2O_3 addition resulted in the increase of Lewis acid sites, however, a slight decrease was observed for Ce_2O_3 addition. From the above analysis of acid sites, the increment for Brønsted acid sites is higher than that for Lewis acid sites; and the increment for moderately strong and super Lewis acid sites decreases in the order: $La_2O_3 > Yb_2O_3 > Ce_2O_3$.

3.5. H_2-TPR behaviour

TPR profiles of the PSZA and RE_2O_3-promoted PSZA catalysts were shown in Fig. 3. Only one peak appeared in these four traces. It was ascribed to the reduction of sulfate ions [6]. In addition, no peak was detected at temperature around 200 °C that usually corresponds to the reduction of Pt oxide to metallic state [6]. PtOx is rather easy to be reduced. The possible reason for this is PtOx reduction was concurrently taken place with reduction of sulfate, because the TPR peak is rather wide ranging from 250 °C to 600 °C, PtOx reduction falls in this range. The differences between the H_2-TPR profiles reflected the effect of RE_2O_3 introduction on the reduction behaviors of the sulfates of the samples. It was given from Fig. 3 that the reduction temperature was 490.8 °C for PSZA, 478.8 °C for PSZAC, 458.3 °C for PSZAL and 457.7 °C for PSZAY. Therefore, RE_2O_3-promoted PSZA catalysts had lower H_2-TPR reduction temperature, which indicated the positive effect of RE_2O_3 to reduction behaviors.

3.6. Catalytic activity test

The *n*-hexane hydroisomerization reactions were performed over PSZA and RE_2O_3-promoted PSZA catalysts at the temperature ranging from 170 °C to 250 °C. The conversion and iso-hexane yields were given in Fig. 4. RE is lanthanum, cerium and ytterbium in our work. The *n*-hexane overall conversion, shown in Fig. 4(a), enhanced with increasing reaction temperature, being higher for RE_2O_3-promoted PSZA catalysts than that for PSZA, and the conversion was decreasing in the order as: PSZAL > PSZAY > PSZAC > PSZA. The difference was more marked at a reaction temperature lower than 220 °C. The iso-hexane yield decreasing under a temperature lower than 220 °C in the order as: PSZAL > PSZAY > PSZAC > PSZA, shown in Fig. 4(b). Above 200 °C, the iso-hexane yields over RE_2O_3-promoted PSZA catalysts decreased due to cracking. However, the La_2O_3 promoted catalyst showed the highest iso-hexane yield at 220 °C. These results showed that introduction of RE_2O_3 would enhance the *n*-hexane hydroisomerization activity; the promotion on the catalytic activity decreased in the order as: $La_2O_3 > Yb_2O_3 > Ce_2O_3$.

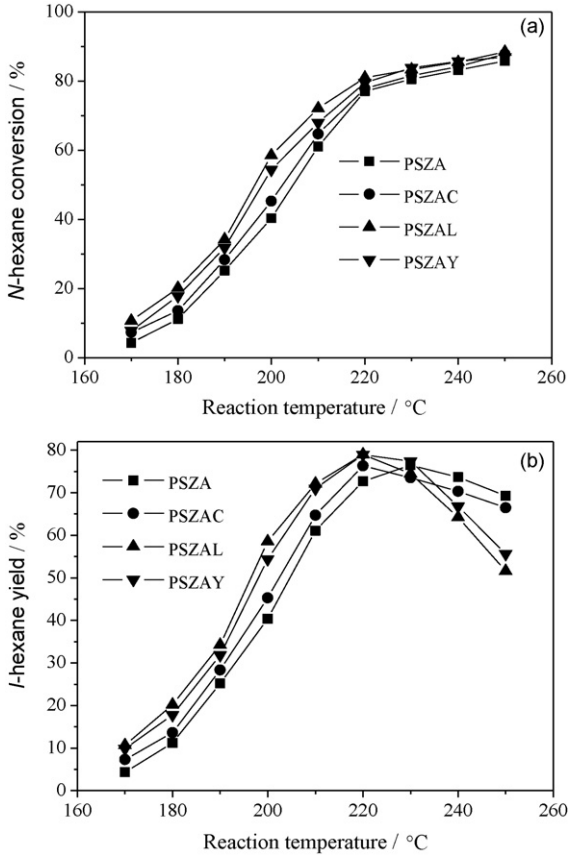

Fig. 4. Effect of reaction temperature on *n*-hexane hydroisomerization over two catalysts (catalyst loading = 1.0 g; WHSV = 1.0 h^{-1}; 2.0 MPa; H_2:n-C_6 = 5:1).

It has been reported that an abundance of surface sulfate species resulted in an increase in surface active sites on the same series of catalysts [16]. Together with TG measurements, it was clear that the introduction of RE_2O_3 into PSZA led to higher sulfates content on the catalysts. It would increase the active sites and thus enhance the catalyst activity as shown in Fig. 4. Moreover, moderately strong and super Lewis acid sites in SZ catalysts would play important roles in catalytic hydroisomerization activity.

The differences in the sulfate reduction ability between the samples, however, might not result from platinum behaviours itself, because PSZA was promoted by different RE_2O_3, whereas the other catalyst preparation procedures are the same. It is supposed that the lower the peak temperature of reduction of surface sulfates on the catalysts is, the more active the sulfates would be, and which would lead to more active sites as shown in Fig. 3 and Table 2. Therefore it was postulated that the differences would come from the surface property differences of the samples after RE_2O_3 promotion, especially their surface acid properties. In H_2-TPR tests, there were possibilities that the stronger the sample surface acid, the stronger its ability to obtain electron and thus the easier, its sulfate reduction by Pt action.

3.7. Catalytic stability of catalysts

To examine the effect of RE_2O_3 on catalyst life, these four catalysts were tested in *n*-hexane hydroisomerization in a microreactor system for 72 h on stream. A hydrogen to hexane molar ratio of 10 was used to provide a more pronounced hydrogenation con-

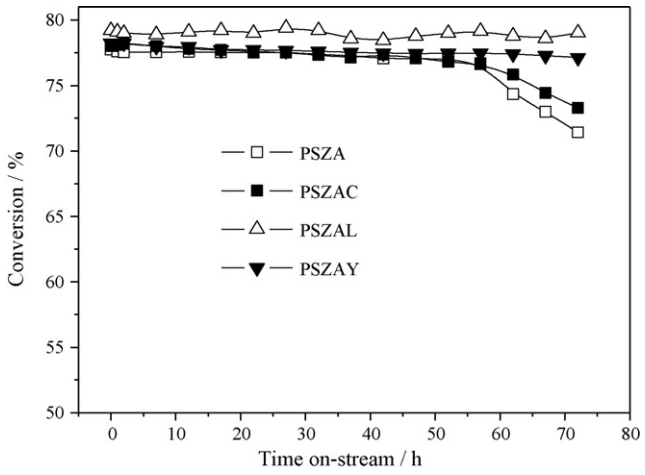

Fig. 5. Time on stream curves of catalysts.

dition in order to study the sulfates reduction loss. Results were shown in Fig. 5 (catalyst loading = 1.0 g; WHSV = 1.0 h^{-1}; 2.0 MPa; H_2:n-C_6 = 10:1), where only overall conversion was given, because the selectivity for iso-hexanes remained 100% during the reaction of 72 h. It was seen that the conversion over PSZA rapidly dropped from 77.75% at the initial stage to 71.43% after 72 h. Whilst for PSZAL, the conversion was slightly decreased from 79.20% to 79.03%; for PSZAY, the conversion was decreased from 78.25% to 77.14%; and for PSZAC, the conversion was decreased from 78.0% to 73.29%. These results indicated that the introduction of RE_2O_3 to PSZA to prepare PSZAY catalysts would enhance the stability of the catalyst in the hydroisomerization reaction, and the promotion for the stability under the hydrogenation condition decreased in the order: $La_2O_3 > Yb_2O_3 > Ce_2O_3$.

3.8. TG analysis of spent catalysts

TG curves for these spent catalysts after 72 h on stream in the microreactor system were given in Fig. 6, where each weight loss below 620 °C was attributed to elimination of adsorbed water and oxidation of deposited coke, whist that above 620 °C was attributed to the decomposition of sulfate species. The corresponding weight losses in the temperature from 620 °C to 1000 °C were respectively 3.84 wt.% for PSZA, 5.51 wt.% for PSZAC, 5.77 wt.% for PSZAL and 5.37 wt.% for PSZAY. Table 3 shows the data obtained together with TG analysis of the fresh catalysts. These data indicated that sulfate

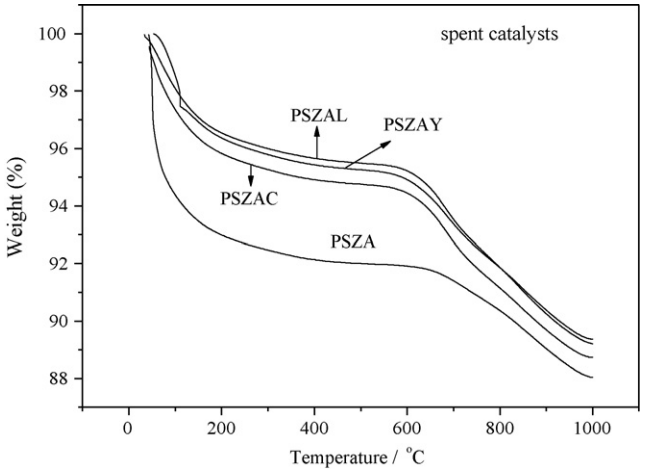

Fig. 6. TG curves of spent catalysts.

Table 3
Sulfates content in catalysts from TG analysis.

Catalyst	Sulfates in fresh catalyst (wt.%)	Sulfates in spent catalyst (wt.%)	Sulfates loss[a] after 72 h reaction (%)
PSZA	4.79	3.84	19.83
PSZAC	6.19	5.51	10.98
PSZAL	6.08	5.77	5.10
PSZAY	5.70	5.37	5.79

[a] Sulfates loss = (sulfates in fresh catalyst – sulfates in spent catalyst)/sulfates in fresh catalyst.

loss after 72 h on stream was 19.83% for PSZA, 10.98% for PSZAC, 5.10% for PSZAL and 5.79% for PSZAY, and the promotion on the sulfates stability decreased in the order: $La_2O_3 > Yb_2O_3 > Ce_2O_3$. These results demonstrated that RE_2O_3 addition to PSZA alleviated the loss of sulfate species and thus improved the hydroisomerization stability of the catalysts.

3.9. Crystalline structures of the spent catalysts

When the sulfate ions were incorporated into $Zr(OH)_4$, they must link hydroxyl ions. Therefore, in the calcination step, condensation among hydroxyl ions was hindered and thus catalyst sintering was alleviated. Moreover, crystallization of ZrO_2 was also retarded by their strong effect to attract electrons [6]. As has been described above, the sulfates loss at some extent was observed on the spent catalysts. It must affect crystalline structures.

As shown in Fig. 7, the XRD patterns of the spent PSZA catalyst (designated as s-PSZA) appeared a sharp peak at $2\theta = 28°$ that was attributed to ZrO_2 monoclinic phase, demonstrating the decrease in tetragonal structure; and the XRD patterns of the spent PSZAC catalyst (designated as s-PSZAC) appeared a very low peak at $2\theta = 28°$ that was attributed to ZrO_2 monoclinic phase; and a lower peak at $2\theta = 28°$ which almost was neglected, appeared for the XRD patterns of the spent PSZAY catalyst (designated as s-PSZAY). On the other hand, this peak was not observed in the XRD pattern of the spent PSZAL (designated as s-PSZAL). Compared to the changes in the sulfate loss and stability behaviors of PSZA and RE_2O_3-promoted PSZA catalysts, the introduction of RE_2O_3 had favorable effect on the sulfates retention, resulting in more stable active crystalline structures, and thus higher stability in the hydroisomerization reactions; and among the three RE_2O_3, La_2O_3 has the best promotion effect.

3.10. XPS analysis of sulfates on the spent catalysts

One very important reason of SZ catalysts deactivation was attributed to a loss of sulfates [28,29]. Sulfate was the only major component in the S 2p spectrum. S 2p binding energy (BE) spectra of the four spent catalysts were shown in Fig. 8. BE ~ 162 eV was assigned to S^{2-}, BE ~ 167 eV assigned to S^{4+}, and BE ~ 169.5 eV assigned to S^{6+} [30]. In Fig. 8, the S 2p BE peaks of the spent catalysts are wide, and the peak at the half width is marked, and the value for the spent catalysts are respectively 167.93 eV for s-PSZA, 167.53 eV for s-PSZAC, 168.15 eV for s-PSZAL and 167.63 eV for s-PSZAY, which indicated that the peak values at the half width were in the range of S^{6+} species (BE 167–169.5 eV). It was seen from Fig. 8 that the appearance of S^{2-} could be close to the noise limit; and S^{4+} species (BE ~ 167 eV) was detected by XPS in the S 2p region of the four spent catalysts; and S^{6+} species (BE 167–169.5 eV) among the sulfates on the four spent catalysts was still most major.

The reduction product of the sulfates would be SO_2, and partly escape from the catalyst surface [31]. XPS showed almost unchanged sulfate peaks, and it suggests the loss of S^{6+} sulfate be the relative small. If it is accepted that not all SO_4 groups were active in isomerization [32], it can be obvious that the few, highly active sulfate groups were most affected by this reduction. Thus, in spite

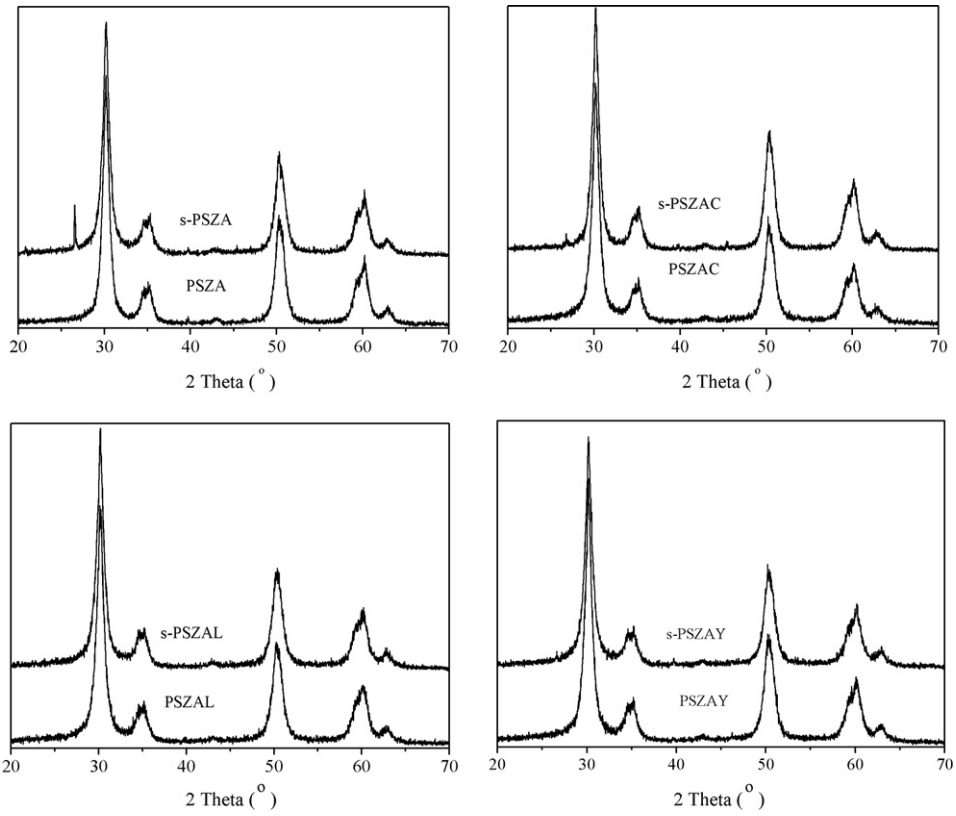

Fig. 7. XRD patterns of the fresh and spent catalysts.

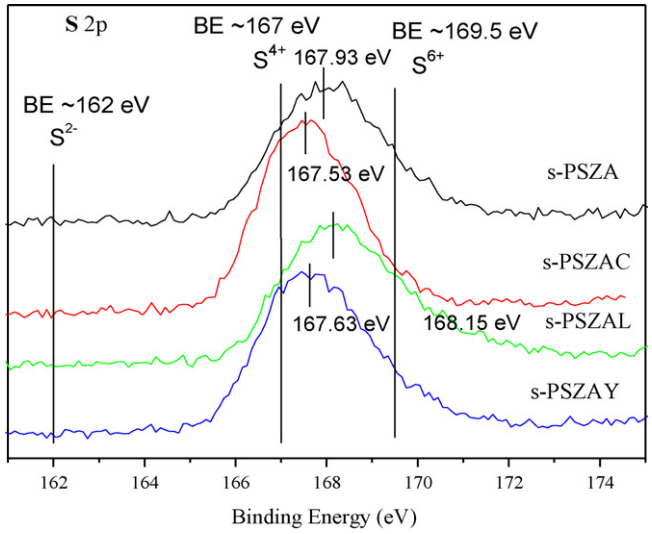

Fig. 8. S 2p binding energy of the spent catalysts.

of the minor loss of S, the crucial sites must have suffered most. This sulfur loss may be the reason why a subsequent sulfidation of the deactivated sulfated zirconia restored its activity [33]. Hence, the amount of the most active sulfate entities decided the overall amount of *n*-hexane transformed, their reduction being, perhaps, retarded by the RE_2O_3 addition to PSZA.

4. Conclusions

The introduction of RE_2O_3 enhanced the *n*-hexane hydroisomerization activity, the promotion on the catalytic activity decreased in the order as: $La_2O_3 > Yb_2O_3 > Ce_2O_3$. RE_2O_3 species have been well dispersed and the crystalline phase structures of PSZA were kept unchanged after modification by rare earth RE_2O_3. The introduction of RE_2O_3 into the catalyst resulted in a higher sulfates content that would alleviate the catalyst sintering and obtain higher catalyst surface area. From analysis of acid sites for PSZA and RE_2O_3-promoted PSZA catalysts, the increment for Brønsted acid sites was higher than that for Lewis acid sites; and the increment for moderately strong and super Lewis acid sites decreased in the order: $La_2O_3 > Yb_2O_3 > Ce_2O_3$. RE_2O_3-promoted PSZA catalysts had lower H_2-TPR reduction temperature.

The catalytic stability experimental results indicated that the introduction of RE_2O_3 to PSZA to prepare PSZAY catalysts would enhance the stability of the catalyst in the hydroisomerization reaction, and the promotion for the stability under the hydrogenation condition decreased in the order: $La_2O_3 > Yb_2O_3 > Ce_2O_3$.

The characterization of the spent PSZA and RE_2O_3-promoted PSZA catalysts showed: RE_2O_3 addition to PSZA alleviated the loss of sulfate species, resulting in more stable active crystalline structures, and thus improved the hydroisomerization stability of the catalysts; and La_2O_3 promotion effects were the highest among the three rare earth oxides. In addition, XPS characterization for the spent catalysts showed during *n*-hexane hydroisomerization reaction a relative small amount of S^{6+} species was reduced to S^{4+}, and the amount of the most active sulfate entities decided the overall amount of *n*-hexane transformed, their reduction being, perhaps, retarded by the RE_2O_3 addition to PSZA.

Acknowledgement

We would like to thank the financial supports from the key international cooperative research projects by National Ministry of Science and Technology, PR China (No. 2004CB720603).

References

[1] L.J. McPherson, in: G.D. Hobson (Ed.), Modern Petroleum Technology, 5th ed., The Institute of Petroleum/John Wiley & Sons, London, 1984.
[2] I.E. Maxwell, Catal. Today 1 (1987) 387.
[3] G.A. Olah, S.K. Prakash, J. Sommer, Superacids, Wiley, New York, 1985.
[4] T. Kimura, Catal. Today 81 (2003) 57.
[5] M. Hino, K. Arata, J. Chem. Soc., Chem. Commun. 3 (1980) 851.
[6] X.M. Song, A. Sayari, Catal. Rev. Sci. Eng. 38 (1996) 320.
[7] T.K. Cheung, B.C. Gates, Top. Catal. 6 (1998) 41.
[8] G.D. Yadav, J.J. Nair, Micropor. Mesopor. Mater. 33 (1999) 1.
[9] K. Arata, Adv. Catal. 37 (1990) 165.
[10] A. Corma, Chem. Rev. 95 (1995) 559.
[11] M.A. Coelho, D.E. Resasco, E.C. Skabwe, R.L. White, Catal. Lett. 32 (1995) 256.
[12] A. Jatia, C. Chang, J.D. Macleod, T. Okubo, M.E. Davis, Catal. Lett. 25 (1994) 21.
[13] V. Adeeva, J.W. de Haan, J. Ja¨nchen, G.D. Lei, V. Schunemann, L.J.M. van de Ven, W.M.H. Sachtler, R.A. van Santen, J. Catal. 151 (1995) 364.
[14] J.C. Yori, J.M. Parera, Appl. Catal. A 147 (1996) 145.
[15] Z. Gao, Y.D. Xia, W.M. Hua, C.X. Miao, Top. Catal. 6 (1998) 101.
[16] W.M. Hua, Y.D. Xia, Y.H. Yue, Z. Gao, J. Catal. 196 (2000) 104.
[17] V.M. Akhmedov, S.H. Al-Khowaiter, Catal. Rev. 49 (2007) 33.
[18] W.M. Hua, A. Goeppert, J. Sommer, J. Catal. 197 (2001) 406.
[19] R. Olindo, A. Goeppert, D. Habermacher, J. Sommer, F. Pinna, J. Catal. 197 (2001) 344.
[20] M. Haouas, S. Walspurger, J. Sommer, J. Catal. 215 (2003) 112.
[21] M. Haouas, S. Walspurger, F. Taulelle, J. Sommer, J. Am. Chem. Soc. 126 (2004) 599.
[22] P. Canton, R. Olindo, F. Pinna, G. Strukul, P. Riello, M. Meneghetti, G. Cerrato, C. Morterra, A. Benedetti, Chem. Mater. 13 (2001) 1634.
[23] W. Wang, J.H. Wang, C.L. Chen, N.P. Xu, C.Y. Mou, Catal. Today 97 (2004) 307.
[24] S.Y. Kim, J.G. Goodwin, D. Galloway, Catal. Today 63 (2000) 21.
[25] C.R. Vera, C.L. Pieck, K. Shimizu, J.M. Parera, Appl. Catal. A 230 (2002) 137.
[26] J.A. Moreno, G. Poncelet, Appl. Catal. A: Gen. 210 (2001) 151.
[27] W. Stichert, F. Schüth, S. Kuba, H. Knözinger, J. Catal. 198 (2001) 277.
[28] K. Ebitani, J. Konishi, H. Hattori, J. Catal. 130 (1991) 257.
[29] M.T. Tran, N.S. Gnep, G. Szabo, M. Guisnet, Appl. Catal. A 171 (1998) 207.
[30] G. Resofszki, M. Muhler, S. Sprenger, U. Wild, Z. Paál, Appl. Catal. A 240 (2003) 71.
[31] A. Ghenciu, D. Fărcasiu, J. Mol. Catal. 109 (1996) 273.
[32] J. Zhao, G.P. Huffman, B.H. Davis, Catal. Lett. 24 (1994) 385.
[33] C. Morant, J.M. Sanz, L. Galán, L. Soriano, F. Rueda, Surf. Sci. 218 (1989) 331.